Applied Catalysis A: General 485 (2014) 40–50

Contents lists available at ScienceDirect

Applied Catalysis A: General

journal homepage: www.elsevier.com/locate/apcata

Copper ion substituted hercynite ($Cu_{0.03}Fe_{0.97}Al_2O_4$): A highly active catalyst for liquid phase oxidation of cyclohexane

Rajib Mistri[a,1], Sayantani Maiti[a], Jordi Llorca[b], Montserrat Dominguez[b], Tapas Kumar Mandal[c], Paritosh Mohanty[d], Bidhan Chandra Ray[a], Arup Gayen[a,*]

[a] Department of Chemistry, Jadavpur University, Kolkata 700032, India
[b] Institut de Tècniques Energètiques and Centre for Research in Nanoengineering, Universitat Politècnica de Catalunya, 08028 Barcelona, Spain
[c] Department of Chemistry, Indian Institute of Technology Roorkee, Roorkee 247667, India
[d] Department of Applied Science and Engineering, Indian Institute of Technology Roorkee, Saharanpur Campus, Saharanpur 247001, India

ARTICLE INFO

Article history:
Received 30 January 2014
Received in revised form 24 June 2014
Accepted 20 July 2014
Available online 28 July 2014

Keywords:
Spinel
Copper substitution
Solution combustion
Cyclohexane oxidation
Ionic interaction

ABSTRACT

Copper ion substituted MAl_2O_4 (M = Mg, Mn, Fe, Ni and Zn) spinels, $Cu_xM_{1-x}Al_2O_4$ (x = 0.03 and 0.05), have been synthesized by a single step solution combustion method. Of the various compositions studied the 3 at.% copper ion substituted hercynite, $Cu_{0.03}Fe_{0.97}Al_2O_4$, reported here for the first time, is shown to be much more active (~92% conversion with ~99% selectivity) than other spinel analogues towards liquid phase oxidation of cyclohexane in acetonitrile with H_2O_2 as oxidant in air. Powder XRD analyses have revealed formation of pure hercynite phases. The least-square refined lattice parameters obtained from XRD data together with microstructural data by HRTEM have indicated copper ion substitution in the spinel lattice. The oxidation state of copper has been established as +2 from XPS analysis and it seem to be primarily substituted in the Fe-site of hercynite. Incorporation of the copper in the spinel structure of $FeAl_2O_4$ leading to an ionic interaction is explained to be responsible for the higher oxidation activity observed over the combustion synthesized catalyst than the corresponding impregnated catalyst which contains finely dispersed CuO crystallites. Effect of recycling (repeated thrice) has shown almost no degradation of activity of the copper ion substituted hercynite. In contrast, the analogous impregnated catalyst has shown appreciable loss of activity in the consecutive cycles due to the presence of dispersed CuO crystallites which can agglomerate with ease and subsequently leach out.

1. Introduction

Selective oxidation of cyclohexane having a relatively inert C–H bond in liquid phase is one of the significant and economical industrial processes [1,2]. The oxidized products of cyclohexane, namely cyclohexanone (K) and cyclohexanol (A) (ketone/alcohol or K–A oil), are the important intermediates for the production of adipic acid and caprolactam, which are used in the manufacture of nylon-6 and nylon-66. The present commercial process for cyclohexane oxidation is carried out at around 150 °C and 1–2 MPa oxygen pressure using chromium oxide as oxidant, nevertheless, only ~4% conversion of cyclohexane and 70–85% selectivity of K–A oil are obtained [2]. Increased demand for these oxidation products in recent years calls for a more efficient and less polluting catalytic process [3–5]. As oxidant, hydrogen peroxide is preferable because of the simplicity of handling and environmental friendly nature of the co-product (water) in the oxidation reaction [6].

The design and development of an efficient catalyst for the oxidation of cyclohexane with hydrogen peroxide as an oxidant is very attractive for the researchers. Among the catalytic studies Ag/TiO_2 [7], V_2O_5–TiO_2 [8], nanoporous Mn(II), Co(II), Ni(II) and Cu(II) complexes [8–10] and porous solids including the TS-1, transition metal (Cr, V, Co, Ti, Ce, Mo etc.) doped MCM-41 [11–14] show good activity towards this oxidation reaction. Many attempts have also been made to develop the catalytic process by using molecular oxygen in absence of any solvent over mesoporous Cu-SBA-15 [15], bifunctionalized hexagonal mesoporous silica (CoPh-HMS) [16] and multifunctional mesoporous iron oxide nanoparticles [17]. However, the majority of these reported catalysts are based on silicates–aluminates molecular sieves and their synthesis condition is extreme and time consuming. Although considerable efforts have been made, cyclohexane oxidation continues to be a challenge [18]. In addition, leaching of active metal from the catalyst has been

* Corresponding author. Tel.: +91 33 2457 2767; fax: +91 33 2414 6223.
E-mail addresses: agayenju@yahoo.com, gayen.arup@gmail.com (A. Gayen).
[1] Present address: Achhruram Memorial College, Jhalda 723202, India.

http://dx.doi.org/10.1016/j.apcata.2014.07.027
0926-860X/

generally observed in most systems. Therefore, it is of great practical interest to develop a more efficient, easily separable, reusable and environment friendly catalyst for the oxidation process.

Spinel type transition metal oxides is a class of chemically and thermally stable materials. These materials have attracted much attention in both fundamental and applied research because of their versatile applications and excellent catalytic properties [19–26]. Binary and ternary oxides possessing a spinel structure have attracted much attention due to their remarkable transport, magnetic and catalytic properties. Mixed metal oxide materials are also good alternatives to both zeolites, such as TS-1, TS-2, Ti-MCM-41, V-ZSM-11 and Cu-ZSM-5, and aluminium phenolate for many alkylation reactions [27]. The catalytic effectiveness of this system is due to the ability of the metal ions to migrate between the sublattices without altering the crystal structure [28–30]. This property makes the spinel efficient for many organic transformation reactions and a number of industrial processes [31–35]. To mention a few, styrene oxidation has been carried out over $NiFe_2O_4$, $ZnFe_2O_4$ and $MgFe_2O_4$ [36,37]. $CuFe_2O_4$ is one of the most excellent oxides for simultaneous catalytic removal of NO_x and diesel particulates [38,39].

In the present work, we report the synthesis, characterization and catalytic activity of copper ion substituted MAl_2O_4 (M = Mg, Mn, Fe, Ni and Zn) spinel oxides. Of all the series of formulations studied here, the $Cu_{0.03}Fe_{0.97}Al_2O_4$ has been found to show the highest selective oxidation activity of cyclohexane to K–A oil than other copper ion substituted spinel oxides using hydrogen peroxide in acetonitrile as the solvent under mild reaction conditions. To the best of our knowledge, this is the first report on the synthesis of copper ion substituted hercynite showing excellent oxidation behavior.

2. Experimental

2.1. Preparation of spinel based oxides

Synthesis of pure and copper incorporated spinels was carried out employing a single step solution combustion method in an open muffle furnace kept in a fume hood by the combustion of the corresponding metal nitrate salts with oxalyldihydrazide ($C_2H_6N_4O_2$ (ODH)) as the fuel. Oxalyldihydrazide was prepared by the dropwise addition of diethyl oxalate ($C_2H_6N_4O_2$, Sisco Research Laboratories Pvt. Ltd., 99%) to ice-cooled aqueous solution of hydrazine hydrate ($N_2H_4{\cdot}2H_2O$, Qualizens Fine Chemicals, 99%) [40].

Pure hercynite ($FeAl_2O_4$ and named as FeAl) and several copper ion substituted hercynites ($Cu_xFe_{1-x}Al_2O_4$ (x = 0.01, 0.03, 0.05 and 0.07) and named as CuFeAln (n = 1, 3, 5 and 7)) were prepared. Specifically, the preparation of $Cu_{0.03}Fe_{0.97}Al_2O_4$ involved combustion of the metal nitrates $Al(NO_3)_3{\cdot}9H_2O$, $Fe(NO_3)_3{\cdot}9H_2O$, $Cu(NO_3)_2{\cdot}3H_2O$ with ODH, taken in a molar ratio 2:0.97:0.03:4.485, at the temperature of ignition of the redox mixture (~350 °C). In a typical preparation, 2 g of $Al(NO_3)_3{\cdot}9H_2O$ (Merck India, 99%), 1.0449 g of $Fe(NO_3)_3{\cdot}9H_2O$ (Merck India, 98%), 0.195 mL of 10% $Cu(NO_3)_2{\cdot}3H_2O$ (Merck India, 99%) solution and 1.4134 g of ODH were dissolved in ~30 mL of double distilled water in a borosilicate dish and then transferred to the preheated muffle furnace for combustion. Initially the solution boils with frothing followed by complete dehydration and then combustion took place which was of smoldering type and was associated with a few sparks. The combustion was completed within 2 min. The colour of the as-synthesized material was brown that became darker with the increase of copper loading.

Copper ion substituted other spinels of general composition $Cu_xM_{1-x}Al_2O_4$ (M = Mg, Mn, Ni and Zn; x = 0.03, 0.05 and named as CuMAl3 and CuMAl5, respectively) were prepared by the combustion of stoichiometric amount of the respective metal nitrates with ODH at ~350 °C in a similar manner. The Ni and Mn-samples were black and the other two were white in color.

For comparison, we prepared CuFeAl3 (the best formulation) by the incipient wetness impregnation (IWI) method. For the preparation of the impregnated catalyst, the support (combustion synthesized $FeAl_2O_4$) was first calcined in air at 400 °C for 3 h and then impregnated with an appropriate volume of the aqueous solution of copper nitrate, corresponding to the support pore volume. The sample was then dried overnight at 110 °C, crushed and calcined at 400 °C for 3 h in air to get the catalyst (CuFeAl3IWI).

2.2. Characterization of materials

The synthesized materials have been characterized by XRD, N_2 sorption analysis, HRTEM and XPS. X-ray powder diffraction patterns were collected in a Bruker D8 Advance diffractometer (40 kV, 40 mA) and operated using CuK_α radiation (effective wavelength 1.5418 Å) with a scanning time of 0.4 s $step^{-1}$ and a step size of 0.02° in the range 10–100°.

The N_2 sorption isotherms were measured at −196 °C using Autosorb iQ-MP (Quantachrome Instruments, USA). Before each measurement, the samples were degassed at 300 °C for about 7 h. The specific surface areas were calculated using BET equation over the pressure range of 0.3–0.08 P/P_0.

Microstructural characterization by High Resolution Transmission Electron Microscopy (HRTEM) was performed at an accelerating voltage of 200 kV in a JEOL 2010F instrument equipped with a field emission source. The point-to-point resolution was 0.19 nm, and the resolution between lines was 0.14 nm. The magnification was calibrated against a Si standard. No induced damage of the samples was observed under prolonged electron beam exposure. Samples were dispersed in alcohol in an ultrasonic bath, and a drop of supernatant suspension was poured onto a holey carbon-coated grid. Images were not filtered or treated by means of digital processing, and they correspond to raw data.

Surface characterization was done with X-ray photoelectron spectroscopy (XPS) on a SPECS system equipped with an Al anode XR50 source operating at 150 mW and a Phoibos 150 MCD-9 detector. The pressure in the analysis chamber was always below 10^{-7} Pa. The area analyzed was about 2 mm × 2 mm. The pass energy of the hemispherical analyzer was set at 25 eV and the energy step was set at 0.1 eV. Charge stabilization was achieved by using a SPECS Flood Gun FG 15/40. The sample powders were pressed to self-consistent disks. The following sequence of spectra was recorded: survey spectrum, C 1s, Fe 2p, Cu 2p, Al 2p, Cu LMM Auger and C 1s again to check for charge stability as a function of time and the absence of degradation of the sample during the analyses. Data processing was performed with the CasaXPS program (Casa Software Ltd., UK). The binding energy (BE) values were referred to the C 1s peak at 284.8 eV. Atomic fractions (%) were calculated using peak areas normalized on the basis of acquisition parameters after background subtraction, experimental sensitivity factors and transmission factors provided by the manufacturer.

2.3. Catalytic test

The oxidation of cyclohexane by H_2O_2 was carried out from RT to 80 °C at atmospheric pressure. In a typical reaction, the catalyst (0.05 g), reactant (8 mmol (0.865 mL) cyclohexane (Merck India, 99.5%)), 10 mL acetonitrile (Merck India, 99.5%) and oxidant (24 mmol (2.45 mL) 30% H_2O_2 (Merck India)) were introduced into a 250 mL two-necked round bottom flask. Uniform mixing of the contents was ensured by continuous stirring (rpm = 900) during the course of reaction by a magnetic stirrer. The reaction

Table 1
Cyclohexane oxidation activities of different copper incorporated spinels.[a]

Spinel sample	Conversion (%)	Product selectivity (%)[b]			Conv[c](mol %)	SE[d](mol %)	TON[e]
		A	K	B			
CuMgAl3	46.3	28.7	65.0	6.3	–	–	353
CuMgAl5	48.6	23.7	68.1	8.2	67.3	44.1	225
CuMnAl3	47.3	29.0	63.2	7.8	–	–	435
CuMnAl5	47.5	16.8	65.9	17.3	–	–	258
CuFeAl3	92.3	29.0	69.7	1.3	98.6	61.5	858
CuFeAl5	93.6	29.7	65.4	4.9	100	59.3	524
CuNiAl3	57.9	21.5	76.2	2.3	–	–	542
CuNiAl5	63.6	20.6	72.6	6.8	88.6	44.5	361
CuZnAl3	34.5	31.3	68.7	–	–	–	336
CuZnAl5	32.4	25.6	74.4	–	–	–	191
CuFeAl3IWI	88.1	23.0	69.0	8.0	97.6	55.4	819

[a] Reaction condition (unless stated otherwise): 0.05 g catalyst, 0.865 mL cyclohexane, 10 mL MeCN, 2.450 mL H_2O_2, 70 °C, 4 h.
[b] A = cyclohexanol, K = cyclohexanone and B = byproduct (mostly cyclohexene and lower amount of cyclohexanediol).
[c] Conv (conversion of H_2O_2 in mol %) = consumption of H_2O_2 (including self-decomposition)/initial amount of H_2O_2.
[d] SE (selectivity of H_2O_2 in mol %) = H_2O_2 consumption for K–A oil formation/total consumption of H_2O_2.
[e] Turnover number (TON) = mole of cyclohexane converted per mole of copper corresponding to the nominal amount taken in synthesis.

system initially consisted of two liquid phases–an organic phase containing reactant and solvent and an aqueous phase containing solvent and oxidant. However within a short period of time after the commencement of reaction, the mixture becomes essentially homogeneous.

The homogenized reaction compositions were analyzed using a gas chromatograph (Nucon 5765, New Delhi) using a fused silica capillary column (EC5) of 30 m × 0.25 mm × 0.25 μm film thickness from Alltech and equipped with a FID detector. The injector and detector temperatures were 220 °C and 240 °C, respectively. The initial and final column temperatures were 110 °C and 150 °C, respectively with a temperature programmed rate of 80 °C min^{-1}. The quantitative analysis was done by standard sample injection.

Catalyst recycling was carried over the most active combustion made CuFeAl3 and its corresponding impregnated (CuFeAl3IWI) catalysts only. After each experiment, the reaction mixture was allowed to settle. Then the solution was filtered and the solid residue was washed thoroughly with the solvent. After washing, the solid residue was dried at 110 °C for overnight. The residue was used as catalyst for the next cycles to check the recycling ability of the catalysts.

3. Results and discussion

3.1. Screening of materials

Table 1 lists cyclohexane oxidation activities of 3 and 5 at.% copper ion substituted spinel oxides. Oxidation activity of copper varies with the variation of M-site cation of the MAl_2O_4 spinel in the following order: Fe > Ni > Mg ≈ Mn > Zn. It is obvious that the CuFeAl3 sample shows much higher reactivity (~92% conversion; cyclohexanone being the major product in each case) and K–A oil (K + A) selectivity (~99%) than the other spinels (see Table 1). The conversion is less than 64% in all other samples and K–A oil selectivity is below 94% except the Zn-spinel that shows 100% K–A oil selectivity but with the lowest conversion, just about 32%. The byproduct (mostly cyclohexene and a lower amount of cyclohexanediol) selectivity was limited to 17%. The much higher oxidation behavior of copper ion substituted hercynite ($Cu_{0.03}Fe_{0.97}Al_2O_4$) indicates much improved promotion effect of $FeAl_2O_4$ spinel than the other spinels studied here. Further studies were thus carried over this spinel only.

Fig. 1(a) shows the cyclohexane conversion as well as selectivity of pure hercynite and various copper ion substituted hercynites, $Cu_xFe_{1-x}Al_2O_4$ (x = 0.01–0.10). Interestingly, the pure hercynite ($FeAl_2O_4$ spinel) shows a conversion of 15%. Maximum conversion and selectivity is achieved at a Cu loading of 3 at.% on $FeAl_2O_4$ – the conversion increases dramatically by more than six times with respect to pure spinel. The 5 at.% Cu loaded sample gave similar conversion but with a bit lower selectivity. Further increase in copper content caused a decrease in cyclohexane conversion as well as K–A oil selectivity (see Fig. 1(a)). Hence we chose CuFeAl3 as the best formulation made via combustion route for other studies.

The effect of temperature on the oxidation of cyclohexane was studied by varying the temperature from 32 to 80 °C over the CuFeAl3 catalyst and the results are shown in Fig. 1(b). At room temperature (32 °C) cyclohexane was not oxidized, showing no reactivity of the catalyst. But an increase of the reaction temperature by just 8 °C results in a sharp increase in the conversion (~70%) as well as selectivity of K–A oil (~95%). Further rise in temperature by 10 °C increases the conversion nearly by 20% which increases slightly (~92%) at 70 °C. The conversion decreases marginally to ~87% when the reaction temperature was increased to 80 °C. The above data indicate that the competition between the products and byproducts occurs above 70 °C. Moreover, an increased self-decomposition of hydrogen peroxide at the higher temperatures results in lower conversion. Thus 70 °C has been chosen as the optimum temperature for the selective oxidation of cyclohexane under our reaction conditions.

Cyclohexane conversion over CuFeAl3 as a function of time at 70 °C is presented in Fig. 1(c). Appreciable oxidation (~17% conversion) starts only after ~60 min. Initially the rate increases slowly leading to ~36% conversion after ~120 min and then rapidly, giving ~80% conversion in ~180 min. Maximum activity (~92% conversion with ~99% K–A oil selectivity) is reached after ~240 min, which remains constant afterwards.

The CuFeAl3 catalyst also shows a comparatively higher oxidation activity than the corresponding impregnated catalyst (CuFeAl3IWI) that gave a maximum cyclohexane conversion of ~88% (see Table 1). This suggests solution combustion as a better and simpler method than impregnation to prepare the spinel catalyst for cyclohexane selective oxidation.

3.2. Effect of H_2O_2 concentration on the cyclohexane oxidation behavior of CuFeAl3

The concentration of H_2O_2 can have a marked influence on the oxidation of cyclohexane. The effect of H_2O_2 concentration was studied by keeping the amount of cyclohexane constant (1 mL or 8 mmol) over CuFeAl3 at 70 °C in acetonitrile. No oxidation products were observed without the use of H_2O_2. Even use of half the stoichiometric molar ratio of oxidant resulted in a mere conversion

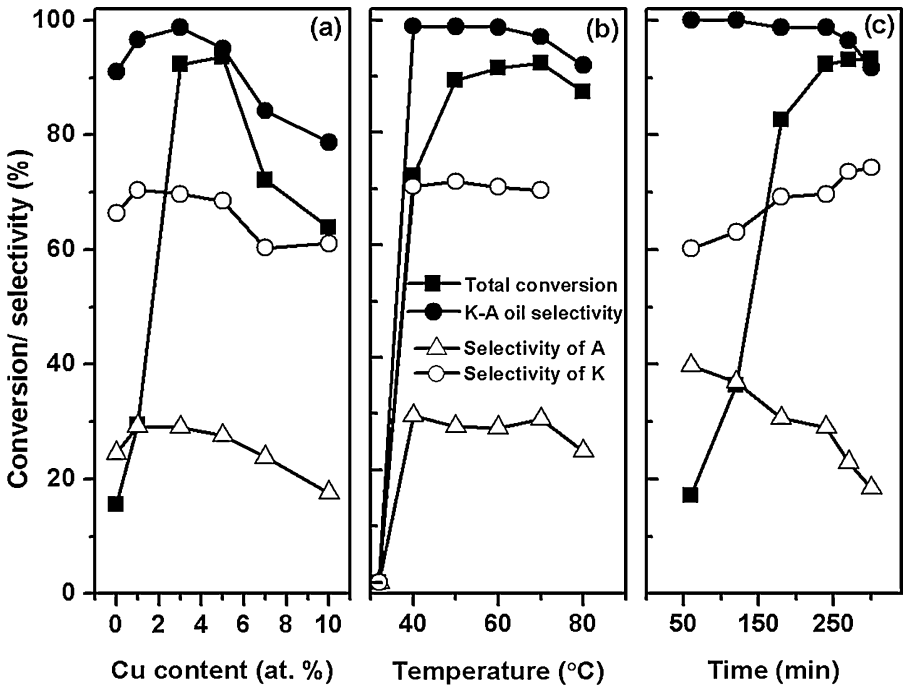

Fig. 1. Cyclohexane oxidation activities of (a) different copper containing $FeAl_2O_4$ spinel oxides (T = 70 °C and time = 4 h), (b) CuFeAl3 at different temperatures (time = 4 h) and (c) CuFeAl3 as a function of time (T = 70 °C). Reaction conditions: 0.05 g catalyst, 0.865 mL cyclohexane, 10 mL MeCN, 2.45 mL H_2O_2.

below 2%. But use of 8 mmol H_2O_2 (stoichiometric amount) leads to 80% oxidation with 98% K–A oil selectivity and the conversion reaches a maximum value of 92% at H_2O_2 concentration of 24 mmol (cyclohexane concentration was 8 mmol). The conversion did not change appreciably with the increase of H_2O_2 concentration from 16 to 32 mmol (or the molar ratio from 1:2 to 1:4). However, K–A oil selectivity decreases beyond use of 32 mmol (1:4 molar ratio) of H_2O_2. The maximum selectivity observed is ~99% for the molar ratio 1:3 (24 mmol of H_2O_2). The selectivity decreases to ~86% in presence of 48 mmol H_2O_2. This decrease in selectivity can be due to the increased formation of water in the reaction mixture, resulting in lowering of solubility, and/or to over-oxidation reactions to the byproducts [41]. Here the result shows that H_2O_2 needed was triple (24 mmol) its theoretical stoichiometry (1:1). This can result from the fact that not all the H_2O_2 takes part in the oxidation process due to its unavoidable self-decomposition under the reaction conditions.

3.3. *Effect of solvent on the cyclohexane oxidation behavior of CuFeAl3*

The solvent usually plays an important role in deciding the activity of catalysts and it also determines the polarity of the medium [42]. But the main action of solvent is still to facilitate the homogeneity of immiscible liquid phases. For example, many solvents have been investigated for the liquid phase oxidation of olefins and alcohols using titanium-containing zeolites as the catalyst [43,44]. We have carried out the oxidation of cyclohexane using various solvents such as acetonitrile, methanol, ethanol and acetic acid over CuFeAl3 and the results are shown in Fig. 2. The activity pattern follows the following order: acetonitrile > acetic acid ≫ ethanol > methanol. Thus, acetonitrile is the best solvent for cyclohexane oxidation over the present CuFeAl3 spinel catalyst with the highest conversion of 92.3% and selectivity of 98.7% to K–A oil. Use of acetic acid as solvent gave a high cyclohexane conversion (68.7%) but the K–A oil selectivity (73.5%) was much lower. Enhanced activity for cyclohexane oxidation in acetic acid has been reported in the literature by Smith et al. [45]. In the media of acetic acid, hydrogen peroxide is more stable and it reduces its self-decomposition by forming peroxyacetic acid. At the same time, as peroxyacetic acid is more hydrophobic than hydrogen peroxide, it acts as a "soft" ligand favoring the oxidation of cyclohexane [46]. Using ethanol or methanol as the solvent, a very low conversion of cyclohexane was observed, just 11% in the former and 7% in the latter.

We believe that acetonitrile acts as a medium serving homogeneity for the liquid phase leading to enhanced activity towards oxidation. Cyclohexane and hydrogen peroxide are mutually soluble in acetonitrile and the reaction products; viz., cyclohexanol and cyclohexanone are not only soluble in the reaction mixture but also can be displaced from the surface of the catalyst as they are formed.

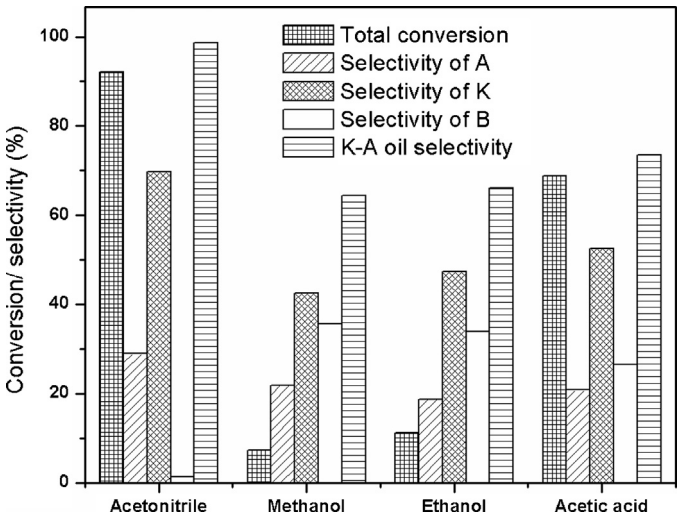

Fig. 2. Influence of solvent on cyclohexane oxidation activities over CuFeAl3. Reaction conditions: 0.05 g catalyst, 0.865 mL cyclohexane, 10 mL solvent, 2.45 mL H_2O_2, 70 °C, 4 h.

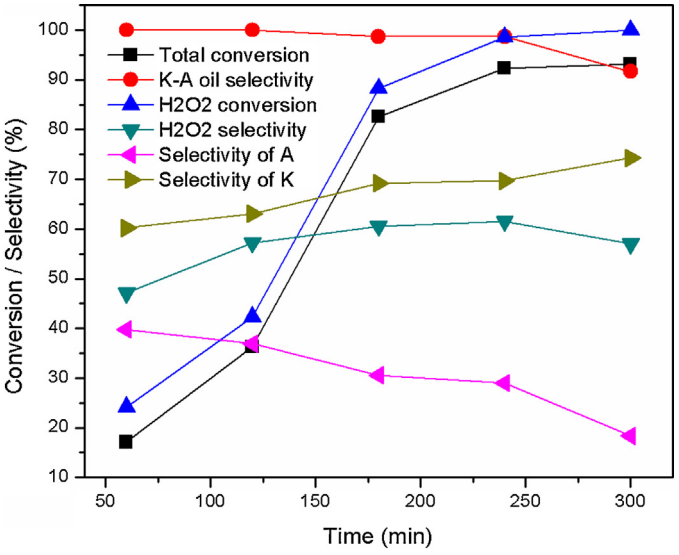

Fig. 3. Time variation of H_2O_2 conversion (Conv) and the corresponding selective decomposition (SE), cyclohexane conversion and K–A oil selectivity (and also individual selectivity values) observed over CuFeAl3. Reaction condition: 0.05 g catalyst, 0.865 mL cyclohexane, 10 mL MeCN, 2.450 mL H_2O_2, 70 °C.

Acetonitrile, an aprotic solvent, can also activate H_2O_2 by forming a perhydroxyl anion to produce a good oxygen transfer intermediate to initiate side chain oxidation at the interface. In addition, the oxidation activity in various solvents can also be related to the effect of H_2O_2 consumption in its self-decomposition as discussed below.

3.4. Effects of H_2O_2 decomposition for cyclohexane oxidation

The selective decomposition of H_2O_2 plays an important role in assessing catalytic activity as well as selectivity. To understand these we tested the mol percentages of H_2O_2 consumption and its selective decomposition under various heads. These include (i) study of the temperature dependence of H_2O_2 decomposition over CuFeAl3, (ii) comparison of H_2O_2 decomposition effects over CuFeAl3 with those over CuFeAl5, CuFeAl3IWI, CuNiAl5 and CuMgAl5 catalysts and (iii) study of H_2O_2 decomposition in different solvents over CuFeAl3. An iodometric titration was used to determine the amount of H_2O_2 consumed for cyclohexane oxidation. It is to be noted that the higher the percentage of H_2O_2 decomposition during the entire course of oxidation, the higher will be the cyclohexane conversion but an initial high H_2O_2 decomposition will lead to nonselective decomposition of H_2O_2. A high percentage of H_2O_2 decomposition with low initial decomposition favors the effective utilization of H_2O_2 and thus enhances the rate of oxidation reaction [47].

During initial stages (up to 2 h) of reaction, H_2O_2 conversions were low (10–30 mol%) but the selectivity of H_2O_2 conversion were high (55–59 mol%) at lower temperatures (up to 50 °C) over CuFeAl3 (see Table S1). The conversions increased with the increase of temperature but with certain loss of selectivity. The competition between H_2O_2 conversion and its selective decomposition is decided to be optimum at 70 °C and after 4 h of oxidation (see Table S1). The time dependence of H_2O_2 conversion and selectivity together with cyclohexane conversion and K–A oil selectivity over CuFeAl3 shows the optimum H_2O_2 conversion to be 98.6% with 61.5% selectivity (see Fig. 3).

It is noteworthy to mention here that the H_2O_2 selective decomposition over CuFeAl3 is the highest (61.5 mol%) when compared with the values obtained over CuFeAl5 (~59 mol%), CuFeAl3IWI (55 mol%), CuNiAl5 (44.5 mol%) and CuMgAl5 (~44 mol%) after 4 h of oxidation (see Tables 1 and S1). These data clearly suggest that the CuFeAl3 catalyst utilizes the oxidant most effectively which is reflected in the cyclohexane conversion as well as K–A oil selectivity values observed over these five formulations.

Acetonitrile showed the minimum H_2O_2 conversion (24.2 mol%) after 1 h of reaction which increased up to 98.6 mol% after 4 h. This is the maximum amount of H_2O_2 conversion observed in our study when compared to other solvents (see Table S2). For example, acetic acid also showed H_2O_2 conversion similar to acetonitrile with an initial decomposition of 26.5 mol% and an increase up to 89.2 mol% after 4 h of reaction. In methanol and ethanol the H_2O_2 conversion was initially moderate (32–34 mol%) and then it increased gradually with the progress of oxidation to about 82 mol%. The initial (first hour) selectivity of H_2O_2 conversion are very low, ~5 mol% and ~3 mol% respectively in ethanol and methanol. Continuation of oxidation up to 4 h leads to only a little gain in selectivity. The mol percentages of selective H_2O_2 conversion follows the order: acetonitrile (61.5%) > acetic acid (~29%) > ethanol (~9%) > methanol (~6%). This is also the activity order of CuFeAl3 catalyst in the different solvents, acetonitrile being the best solvent showing maximum conversion with maximum selectivity for cyclohexane oxidation under the chosen reaction conditions reported in this study.

The poor peroxide selectivity can account for lower cyclohexane conversion as well as K–A oil selectivity in ethanol and methanol. In these polar protic solvents, the generated hydroxide radical gets additional stability due to H-bond formation and the equilibrium is shifted towards the right increasing the self-decomposition rate. Most of the H_2O_2 is thus lost in its self-decomposition during initial stages. The fraction of hydroxyl radical utilized for K–A oil formation is thus less compared to total H_2O_2 decomposition attributable to low conversion as well as low selectivity. Interestingly, acetonitrile and acetic acid show a higher peroxide selectivity with a high H_2O_2 conversion. Because of the polar aprotic character of acetonitrile, the generated hydroxyl radical does not get stability as in the polar protic solvents. In the medium of acetic acid, H_2O_2 becomes more stable by forming peroxyacetic acid eventually reducing its self-decomposition. Hence loss of H_2O_2 by self-decomposition occurs in a comparatively lower proportion in these two solvents.

3.5. Recycling ability and heterogeneity of CuFeAl3 and CuFeAl3IWI catalysts

In order to differentiate better the two types of (combustion made and impregnated) catalysts and to correlate the activity with the structure we subjected the catalysts to recycling treatments. To do so, the used catalyst was separated from the reaction mixture and dried in air at 110 °C, and then oxidation experiments were performed under the typical reaction conditions used here. The combustion synthesized catalyst (CuFeAl3) was found to maintain its activity in the consecutive cycles (repeated thrice) without any noticeable loss of conversion and K–A oil selectivity. But the IWI catalyst (CuFeAl3IWI) showed decreasing conversion-selectivity pattern in the second cycle itself (~80% conversion with ~86% K–A oil selectivity) that decreased further in the third cycle when a conversion of 73% with 82% selectivity was noted. Thus, the conversion over the IWI catalyst decreases by ~9% in each consecutive cycle with concomitant loss of K–A oil selectivity as well (7–5%).

To check whether cyclohexane oxidation was truly heterogeneously catalyzed or not and to look for any possible metal leaching and involvement of any homogeneously catalyzed contribution, the conventional hot filtration test of Sheldon was carried out over CuFeAl3 and CuFeAl3IWI catalysts. To do so a hot reaction mixture was separated from the catalyst before complete conversion was reached. The catalyst was immediately filtered off through a Gooch

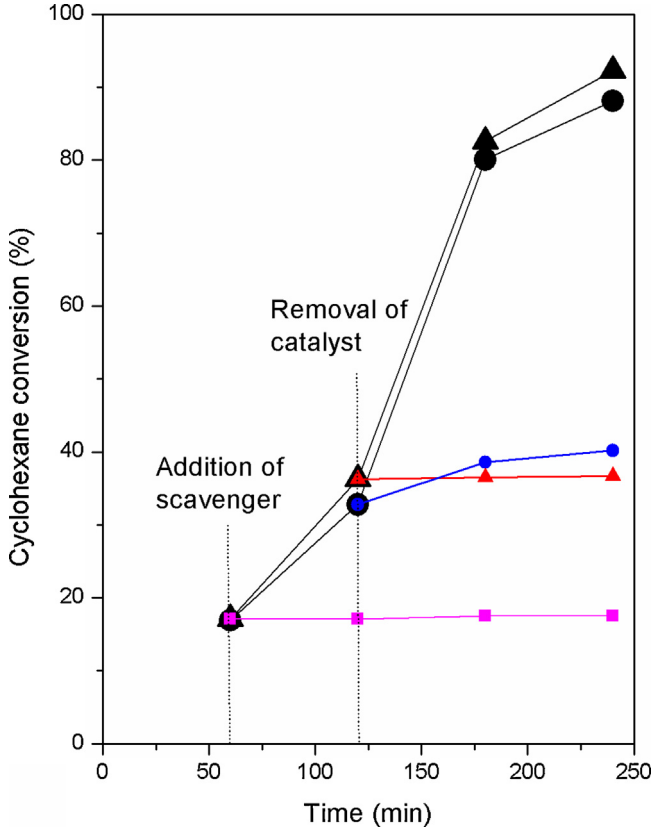

Fig. 4. Cyclohexane conversion as a function of time over CuFeAl3 (▲) and CuFeAl3IWI (●); after removal of catalyst from the reaction mixture (Sheldon's test) for CuFeAl3 (▲) and CuFeAl3IWI (●); after addition of scavenger (quinone) (■) at 70 °C for CuFeAl3.

(G4) after 2 h of oxidation at 70 °C in order to avoid re-adsorption of leached metals, if any, onto the catalyst surface. The filtrate was collected into another preheated reaction flask at the same temperature and the reaction was continued for another 2 h. Gas chromatographic analysis of the reaction aliquot showed essentially no increase in conversion (remains almost constant at 35%) up to 4 h for the combustion synthesized catalyst CuFeAl3 (see Fig. 4) when compared with the time variation of activity pattern of this catalyst. But in case of the IWI catalyst, CuFeAl3IWI, the hot filtration test shows although little but certain increase in conversion during the mentioned timeframe (see Fig. 4). The reaction is, therefore, truly heterogeneous in nature over CuFeAl3 and possibility of metal leaching or decomposition of the catalyst material can be excluded. The certain improvement in conversion even in the absence of catalyst for CuFeAl3IWI confirms that cyclohexane oxidation over this impregnated catalyst is not purely heterogeneous in nature and there is a certain amount of leaching of active metal component to the solution during the progress of reaction. We could not perform Cu-analysis of the reaction crude after catalyst separation by ICP-OES which could have shed more light towards our understanding of the leaching phenomenon.

Findings of above studies imply that the Cu^{2+} ion sites in the spinel lattice are stable enough (do not leach out) towards the oxidation reaction for the combustion synthesized catalyst and hence its activity remains essentially same. Whereas the dispersed CuO crystallites in the impregnated catalyst can grow bigger/agglomerate and escape the catalyst surface during cyclohexane oxidation which results in lower activity in the consecutive cycles as has been observed.

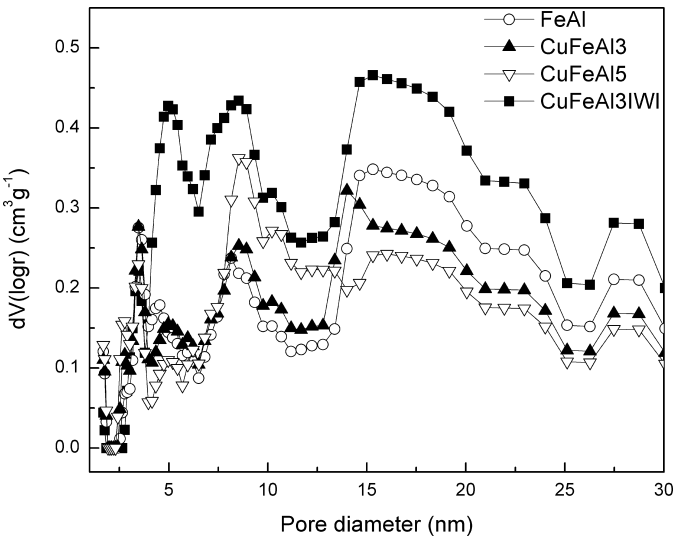

Fig. 5. Pore size distribution of (a) FeAl, (b) CuFeAl3, (c) CuFeAl5 and (d) CuFeAl3IWI samples estimated by the Density Functional Theory (DFT) method from the N_2 sorption of the sample measured at liquid nitrogen temperature.

3.6. Textural studies

We studied the specific surface areas and pore volumes of pure FeAl spinel, the spinel catalysts CuFeAl3 and CuFeAl5 made by solution combustion and CuFeAl3IWI made by impregnation method. The specific surface areas of all these samples calculated from the BET equation are in the range 134–149 $m^2\,g^{-1}$. The specific surface area and pore volume of the pure spinel sample was 139 $m^2\,g^{-1}$ and 0.289 $cm^3\,g^{-1}$, respectively. As expected, on incorporation of 3 at.% and 5 at.% copper in the spinel by the single step solution combustion leads to a slight decrease in the pore volume (from 0.289 $cm^3\,g^{-1}$ in the pure spinel) to 0.277 and 0.270 $cm^3\,g^{-1}$, respectively. However, there is almost ~7% increase in the specific surface area (from 139 $m^2\,g^{-1}$ in the pure spinel) to 149 and 148 $m^2\,g^{-1}$ in the 3 at.% and 5 at.% copper incorporated sample, respectively. This trend of higher specific surface areas with lower pore volume could be explained by studying the pore size distribution (PSD) of these samples. All of these samples have multimodal pore system with the pores centered around 3.2, 8.4 and 16 nm, with a small shoulder around 5 nm (see Fig. 5). However, the populations of these pores are different in different samples. For example, in the pure spinel sample the intensity of the pore centered at 16 nm is maximum and it decreases in regular fashion on increasing the copper incorporation leaving other smaller pores unaffected, which explains the observation of the higher surface areas in these samples. The copper impregnation on $FeAl_2O_4$ leads to an increase of pore volume from 0.289 $cm^3\,g^{-1}$ in the pure spinel to 0.423 $cm^3\,g^{-1}$ in the impregnated catalyst with a marginal decrease in the specific surface area. This may be attributed to the deposition of the copper on the surface of the catalyst without affecting much of the mesopores. The PSD of the impregnated catalyst also shows similar multimodal pore systems centered around 3.2, 5, 8.4 and 16 nm.

3.7. XRD studies

Powder XRD patterns of $Cu_xFe_{1-x}Al_2O_4$ ($x = 0$–0.07) spinels are shown in Fig. 6. Only a faint signature of spinel phase is there for the pure $FeAl_2O_4$ oxide. The peak intensity and hence the crystallinity increases with the increase of Cu-loading from 1 at.% to 7 at.%. It is obvious that the presence of Cu^{2+} in the spinel lattice helps to crystallize the phase – even just 1 at.% Cu in $FeAl_2O_4$ has

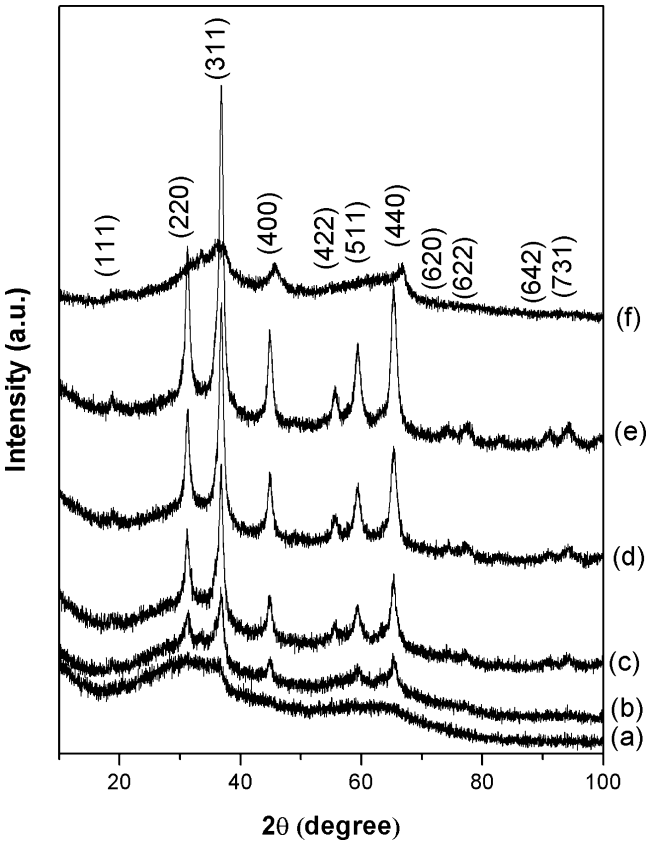

Fig. 6. Powder XRD patterns of (a) FeAl, (b) CuFeAl1, (c) CuFeAl3, (d) CuFeAl5, (e) CuFeAl7 and (f) CuFeAl3IWI.

a dramatic effect on the crystallinity. All the peaks correspond to $FeAl_2O_4$ spinel phase (JCPDS PDF # 34-0192) only. No peak(s) due to Cu–related phase(s) could be detected. The least-square refined lattice parameters of the $Cu_xFe_{1-x}Al_2O_4$ (x = 0.01–0.07) indicate a systematic decrease (8.095(5) Å for 1 at.% to 8.084(1) Å for 5 at.% Cu substituted $Cu_xFe_{1-x}Al_2O_4$) with increase in Cu loading. This contraction of lattice parameter is in agreement with the incorporation of Cu in the Fe site of $FeAl_2O_4$. For the impregnated catalyst, CuFeAl3IWI, the crystallinity is better than the combustion made pure spinel. In the impregnated catalyst, copper is present as CuO finely distributed over the $FeAl_2O_4$ support and probably not incorporated in the spinel lattice. So, copper impregnation in the $FeAl_2O_4$ support has a definitive but minor role towards the crystallinity of the spinel phase in sharp contrast to copper loading effect in combustion derived $Cu_xFe_{1-x}Al_2O_4$ materials obtained in a single step solution combustion method.

3.8. Microstructural studies

A detailed analysis of the microstructure of $FeAl_2O_4$ spinel oxide support and copper ion substituted spinels ($Cu_xFe_{1-x}Al_2O_4$ (x = 0.03–0.07)) were carried out. Fig. 7(a) shows a general view of the FeAl sample, which does contain mostly flakes of the spinel support. These flakes oscillate in size from about 10 to 40 nm. Electron diffraction patterns obtained over several areas of the sample show in all cases spots that define circles at 4.71, 2.88, 2.46, 2.04 and 1.87 Å, which precisely match the (1 1 1), (2 2 0), (3 1 1), (4 0 0) and (3 3 1) crystallographic planes of $FeAl_2O_4$. No other spots are present in the diffraction patterns, thus indicating that the sample only contains the spinel structure. Fig. 7(b) shows a high magnification HRTEM image of the sample. Planes at 2.45 Å are indicated, which correspond to the (3 1 1) crystallographic planes of $FeAl_2O_4$.

Fig. 7(c) shows a general view of the CuFeAl3 sample. It appears that the presence of copper facilitates the formation of hercynite ($FeAl_2O_4$) particles with a narrow size distribution pattern, mostly between 5 and 15 nm. Fig. 7(d) shows an HRTEM image. The FT image enclosed corresponds to the area within the white square. Spots at 2.45 Å correspond to the (3 1 1) crystallographic planes of the spinel structure. It is important to note that no other phase, either crystalline or amorphous, has been detected by HRTEM, suggesting that copper addition to $FeAl_2O_4$ by the solution combustion method results in the incorporation of copper in the spinel structure. Unfortunately, the atomic radius of Fe(II) and Cu(II) are very similar, and the error involved in the analysis of the lattice fringes does not allow for a calculation of the lattice parameter of the spinel structure precise enough to discuss about the substitution of Fe(II) by Cu(II) in the catalyst by HRTEM. However, the XRD results support the incorporation of Cu at the Fe site and also no CuO phase is detected in the HRTEM studies.

The microstructure of catalysts CuFeAl5 and CuFeAl7 is virtually identical to that of CuFeAl3. Fig. 7(e) corresponds to a HRTEM image (of CuFeAl5) which shows the crystalline nature of the sample. In the FT image, spots at 2.45, 4.0 and 2.86 Å correspond to the (3 1 1), (2 0 0) and (2 2 0) crystallographic planes of the spinel structure. The occurrence of lattice fringes at 4.0 Å, which correspond to the (2 0 0) crystallographic planes of the spinel structure – forbidden by symmetry rules – is an indication that copper may be incorporated into the spinel structure. Again, no evidences for the existence of the CuO phase are encountered, in accordance with the fact that copper has entirely incorporated into the spinel structure. This HRTEM observation in conjunction with the refined lattice parameter data strongly supports copper incorporation into the spinel structure in all the $Cu_xFe_{1-x}Al_2O_4$ catalysts. Moreover, it has always been observed that for CuFeAl7, containing the maximum amount of Cu, the lattice fringes are always lower as compared to other samples.

A slight increase in particle size is detected by TEM for the sample CuFeAl3cy2 (after two cycles of cyclohexane oxidation over CuFeAl3 catalyst). Most particles range between 10 and 20 nm after cycling. Interestingly, HRTEM reveals the formation in some cases of steps and twins following the cycling treatment. In Fig. 7(f), two areas enclosed in white squares have been analyzed by FT. In one of them, well-defined spots at 2.45 Å are identified, which correspond to the (3 1 1) crystallographic planes of the spinel structure. In contrast, the other FT shows strips instead of well-defined spots, which are due to structural imperfections of the crystal, as it is evident in the HRTEM image. These imperfections are usually considered much more reactive for catalysis and may originate from reconstruction under reaction conditions. Importantly, cycling in the reaction atmosphere does not remove/leach out the substitutional copper-ions from the spinel lattice. Hence, no variation in activity pattern is expected in the consecutive cycles as has been observed in our experiments.

The sample CuFeAl3IWI prepared by incipient wetness impregnation method contains well-dispersed particles of about 5–10 nm together with flakes with sizes up to 60–70 nm. The sample is constituted by crystalline particles, as shown by HRTEM (Fig. 7(g)–(h)). It is very interesting to note that the lattice fringes recorded in the HRTEM images exhibit values virtually identical to those of the $FeAl_2O_4$ support: 2.04, 2.44-2.46, 4.71 Å (which corresponds to the (4 0 0), (3 1 1) and (1 1 1) crystallographic planes of the spinel structure). In addition, there is a complete absence of the symmetry-forbidden lattice fringes at 4.0 Å corresponding to the (2 0 0) crystallographic planes. This can be interpreted as an evidence of lack of copper incorporation into the spinel structure in the IWI catalyst. No CuO segregated phase is identified by HRTEM in the sample. Then, if no copper incorporation into the spinel structure occurs and no CuO phase is detected, this means that CuO is very well dispersed over the sample, in such a way that escape

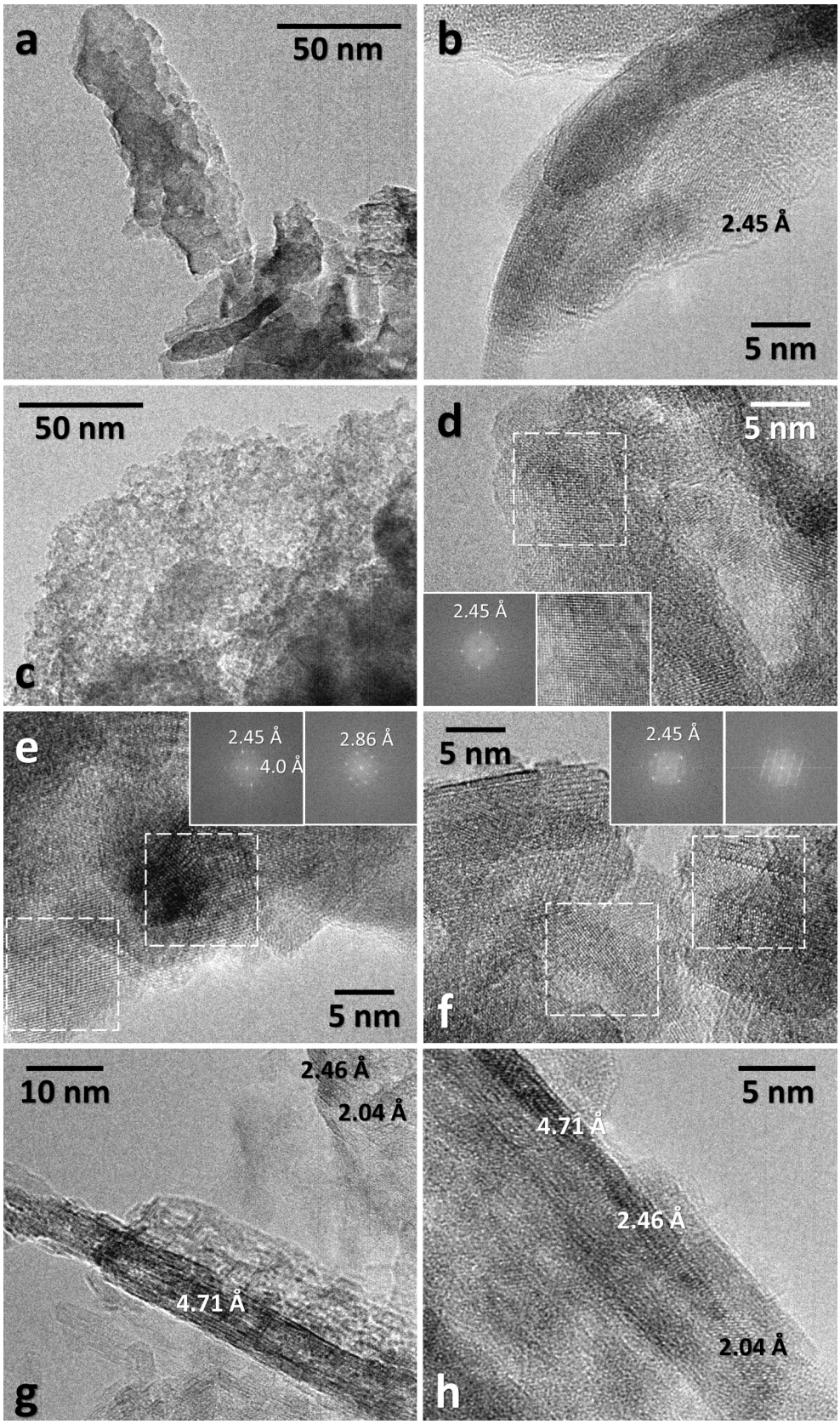

Fig. 7. TEM images of (a and b) FeAl, (c and d) CuFeAl3, (e) CuFeAl5, (f) CuFeAl3cy2 and (g and h) CuFeAl3IWI catalysts.

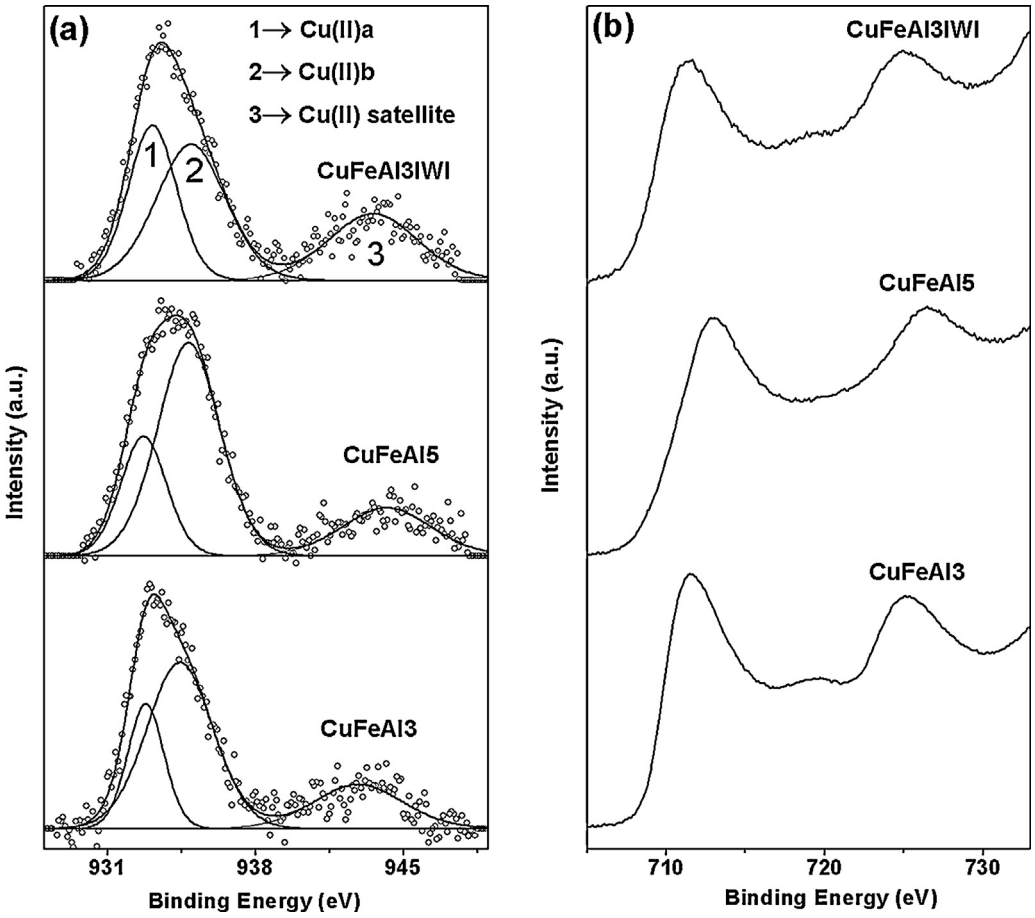

Fig. 8. XPS spectra of (a) Cu $2p_{3/2}$ and (b) Fe 2p regions of CuFeAl3, CuFeAl5 and CuFeAl3IWI catalysts.

HRTEM detection. Possibility of leaching of these dispersed CuO particles over $FeAl_2O_4$ during cycling in the reaction environment is certainly more than the ionically substituted copper in the spinel structure. Thus, the activity of CuFeAl3IWI, with dispersed CuO phase eventually decreases in the consecutive cycles.

3.9. XPS studies

The combustion derived CuFeAl3, CuFeAl5 and impregnated sample CuFeAl3IWI were analyzed by XPS to ascertain the oxidation state(s) of elements present and their surface atomic composition that has important role in catalysis. Apart from the general survey spectra, high resolution spectra for C 1s, Fe 2p, Cu 2p, Al 2p and Cu LMM Auger were recorded and analyzed. Fig. 8 shows the core level regions of Cu 2p and Fe 2p for the different catalysts. Binding energies of copper, iron and aluminium along with the full width at half maximum (FWHM) and surface atomic concentrations of these species for the different catalysts are listed in Table 2. The binding energies for each species match the corresponding ion, Cu(II), Fe(II) and Al(III). For both the combustion synthesized and the impregnated catalysts, there is an enrichment of aluminium on the surface relative to the theoretical composition of the $FeAl_2O_4$ spinel, particularly in the impregnated sample, which exhibits low iron content at the surface (see Table 2). The combustion made samples contain more copper atoms on the surface with respect to the impregnated one. This is in accordance with the speculation that on the impreganted sample (CuFeAl3IWI) there is CuO whereas in the combustion synthesized samples (CuFeAl3 and CuFeAl5), part of iron has been substituted by copper.

Fig. 8 also includes the deconvoluted peaks of Cu $2p_{3/2}$ signal of the combustion synthesized and impregnated catalysts. All components correspond to oxidized Cu. There is one main signal due to Cu(II) species and one satellite signal. The main signal clearly contain two components, indicating that there are two types of Cu(II) sites, named as Cu(II)a and Cu(II)b that closely resembles the core-level binding energies of Cu(II) oxide and Cu(II) hydroxide, respectively [48]. The relative abundances of each Cu(II) site is clearly different between the two types of samples. In particular, the combustion synthesized samples contain a larger signal centered at 934.4–934.8 eV. This is accompanied by a low intensity of the satellite peak. The satellite is more pronounced when there is CuO in comparison to other Cu(II) species [48]. Then, it appears that the component at 932.7–933.1 eV may be due to CuO. This component is more intense for the impregnated

Table 2
Binding energy, FWHM and surface atomic concentration of Fe, Cu and Al of different catalysts.

Catalyst	Peak details	BE (eV)	FWHM (eV)	% At conc.
CuFeAl3	Fe $2p_{3/2}$	711.1	3.57	23.1
	Cu $2p_{3/2}$	933.0	3.79	1.9
	Al 2p	74.3	2.35	75.0
CuFeAl5	Fe $2p_{3/2}$	712.2	4.25	20.1
	Cu $2p_{3/2}$	933.5	4.38	3.0
	Al 2p	74.2	3.32	76.9
CuFeAl3IWI	Fe $2p_{3/2}$	710.8	4.00	6.6
	Cu $2p_{3/2}$	933.9	3.79	1.2
	Al 2p	74.3	2.452	92.2

sample, which exhibits a stronger satellite signal (see Fig. 8(a)). The combustion made samples, with a much weaker satellite line and less intense 932.7 eV signal seems to contain other Cu(II) species than CuO type. We attribute this to the presence of substitutional Cu(II) ions (for Fe ions in the $FeAl_2O_4$ spinel lattice surface) in the combustion made CuFeAl3 and CuFeAl5 samples in conformity with the HRTEM and XRD findings. Thus, all the structural studies indeed support that a part of iron in the spinel has been substituted by copper-ion in the combustion synthesized catalysts.

Finally, the Cu LMM Auger line (spectra not included here) centered at 339 eV suggests presence of only Cu(II) species. This LMM line is particularly useful for detecting Cu(I) species, but there are not. So, from XPS analysis we conclude that both the combustion synthesized and the impregnated samples contain only Cu(II) species – whereas it is mainly substitutional Cu(II) in the combustion synthesized samples, the impregnated sample contain mainly dispersed CuO crystallites.

In the present study, we have looked into the activities of copper ion incorporated hercynite spinels towards oxidation of cyclohexane in liquid-phase. Most importantly, we have correlated the cyclohexane oxidation behavior of the best formulation, 3 at.% Cu over $FeAl_2O_4$, prepared by solution combustion and incipient wetness impregnation methods with the phase composition of these catalysts. Since the nominal composition is the same, surface area being similar and pore systems are of multimodal types there have to be other factors like morphological differences and most presumably the structural differences in them, playing a key role in the higher oxidation activity recorded for the combustion made CuFeAl3 catalyst.

The variation of activity with copper content of the copper loaded hercynite spinels can be related with the surface atomic concentration of substitutional copper ions as obtained from XPS analysis. Out of 3 at.% copper taken in the preparation of CuFeAl3 sample, about 2 at.% remains on the surface of the spinel (see Table 2). In the CuFeAl5 sample, proportion of this surface copper is comparatively less (of the 5 at.% copper taken in the synthesis, 3 at.% remains on the surface). It is postulated that the fraction of ionically substituted copper on the surface of spinel lattice decreases much more beyond 5 at.% copper ion substitution in $FeAl_2O_4$. This leads to a lowered conversion-selectivity pattern towards cyclohexane oxidation from CuFeAl5 onwards. Saturation level of copper on the surface for cyclohexane oxidation is reached at 3 at.% copper ion substitution level. Thus, the CuFeAl3 catalyst shows the best activity behavior.

The activity of the impregnated catalyst is only slightly lower when compared to the corresponding combustion synthesized catalyst (see Table 1) after first 4 h of reaction. This may be due to the presence of very highly dispersed CuO crystallites on the $FeAl_2O_4$ spinel in the IWI catalyst. The sizes of these CuO crystallites are below the detection limit of HRTEM as discussed above. But the recycling experiments over the IWI catalyst show appreciable decrease of activity in the consecutive cycles indicating possible loss/or agglomeration of these dispersed CuO crystallites from the spinel surface. On the contrary, it is the stable ionically substituted copper in the Fe-site of $FeAl_2O_4$ spinel for the combustion synthesized catalyst that plays the key role for cyclohexane oxidation and hence no appreciable change in activity behavior was noted in the consecutive cycles.

Cyclohexane oxidation generally proceeds through a radical pathway in presence of a peroxide oxidant [2]. To examine the mechanism involved in the present case, we performed the oxidation in presence of a radical scavenger (quinone). The radical scavenger was added to the reaction mixture after 1 h of reaction and the progress of reaction was monitored. Cyclohexane oxidation was found to be totally stopped after addition of the scavenger (see Fig. 4). Therefore, we believe that cyclohexane oxidation over the reported catalysts in this study proceeds via a radical mechanism [18,49]. Hydroxide radical is first produced mostly through involvement of $Cu^{2+} \leftrightarrow Cu^{+}$ redox couple that subsequently abstracts hydrogen from the reactant to produce cyclohexyl free radical. This radical is then trapped by O_2 and/or combine with hydroperoxide radical to form cyclohexyl peroxide intermediate which eventually leads to the formation of cyclohexanol and cyclohexanone.

Selvam et al. have reported a Cr-MCM-41 catalyst that showed a maximum cyclohexane conversion of 99% with 93% selectivity to cyclohexanol and cyclohexanone using acetonitrile as solvent at 70 °C under atmospheric pressure in a longer duration of 12 h [13]. But a major decrease in activity was observed in the second cycle (75% conversion with 95% selectivity) and the activity decreased to a lesser extent in the third cycle (72% conversion with 94% selectivity) due to leaching of some active metal during the consecutive cycles. Wang et al. have also reported similar activity pattern over Ce-MCM-41 (95% conversion with 90% selectivity) and they have shown that metal leaching can be controlled by using synergistic effects among doped cerium and mesoporous framework of MCM-41 that helps maintaining the same activity for three consecutive cycles (92–90% conversion with 86–85% selectivity) [9]. The metal leaching has also been reported to be resistant up to four cycles (conversion was lowered by ~2%) with reserve selectivity over [CuL]-NaY zeolites [10]. High cyclohexanol and cyclohexanone yield (58.6% conversion with 100% selectivity) have been reported for $Cu_2P_2O_7$ also and in this case the formation is decreased only by 1-2% in the regenerated catalyst after three cycles [18]. The metal leaching has also been shown to be effectively decreased using vanadium phosphorus oxide (VPO) in the oxidation of cyclohexane (76% conversion with K–A oil selectivity of 100%) using H_2O_2 in acetonitrile at 65 °C in 8 h [5]. Recently Parida et al. have reported Fe(III) Schiff-base complexes incorporated in LDH that gave 100% K–A oil selectivity from cyclohexane oxidation (conversion ~45%) with low metal leaching [49]. Pârvulescu et al. have also reported a 100% selective NaGe-X catalyst showing 66.5% conversion for this reaction at 70 °C in absence of any solvent [50]. The metal leaching problem is shown to be resistant up to three cycles by using highly dispersed CuO into the pore channels of mesoporous SBA-15 for this reaction with oxygen in a solvent free condition [15]. Xu et al. have also reported that metal leaching can be controlled by using bifunctionalized CoPh-HMS-20 catalyst that helps maintaining the same activity for three consecutive cycles [16]. Comparison of the reported catalytic systems with our catalyst thus suggests significantly superior activity behavior of the combustion synthesized catalyst.

The novelty of the present copper ion substituted hercynite catalyst originates from the presence of catalytically active Cu^{2+} ion sites presumably in the surface layers of the $Cu_{0.03}Fe_{0.97}Al_2O_4$ spinel. Our thorough structural studies have unequivocally shown that ionic copper is indeed present in the spinel lattice. An ion being the active site, the predominant interaction is ionic in nature. Ionic copper in the spinel lattice is also shown to be stable enough towards recycling treatments. To our knowledge, most of the catalytic systems available in the open literature report TONs in between 100 and 400 except NaGe-X which shows a TON of 798. The combustion synthesized spinel catalyst, $Cu_{0.03}Fe_{0.97}Al_2O_4$, reported here for the first time have been found to show a high TON of 858 (see Table 1) that remains unaltered in the consecutive cycles due to well-defined structure of the catalyst. Thus, solution combustion synthesis has been shown to be an effective fast methodology to prepare single phase spinel oxide catalyst having excellent oxidation behavior towards organics like cyclohexane.

4. Conclusions

Solution combustion synthesis has been shown to be a very fast novel synthetic route to synthesis of single phase spinel oxides of which $Cu_{0.03}Fe_{0.97}Al_2O_4$ is shown to be a highly efficient catalyst for the oxidation of cyclohexane in acetonitrile at 70 °C. The structural studies have shown ionic substitution of copper in the $FeAl_2O_4$ spinel. The XPS studies have confirmed presence of copper in +2 oxidation state and it is primarily substituted in the Fe-site of the spinel. High surface atomic concentration of copper than the theoretically expected value increases the availability of catalytically active sites. A high conversion of cyclohexane (~92%) with the K–A oil (cyclohexanone-cyclohexanol) selectivity of ~99% is reported over the spinel catalyst. This high activity has been attributed to well defined structure of the catalyst, active copper ion sites and ionic interaction in the $Cu_{0.03}Fe_{0.97}Al_2O_4$ spinel oxide catalyst. Since copper is incorporated as ion in the structure of the $FeAl_2O_4$ spinel, so the possibility of copper leaching is reduced in the combustion synthesized catalyst. The recycling experiments have confirmed this since there was no loss of activity due to these treatments. The nearly similar activity of the impregnated catalyst in its as-prepared form to combustion synthesized catalyst is due to the presence of finely dispersed CuO crystallites over the $FeAl_2O_4$ support. But the impregnated catalyst experienced significant loss of activity after first cycle of oxidation which is attributed to leaching of CuO from the surface of the spinel support.

Acknowledgements

Financial support from the Department of Science and Technology, Government of India, by a grant (SR/S1/PC-28/2010) to AG is gratefully acknowledged. JL is grateful to ICREA Academia program (Generalitat de Catalunya).

Appendix A. Supplementary data

Supplementary data associated with this article can be found, in the online version, at http://dx.doi.org/10.1016/j.apcata.2014.07.027.

References

[1] U. Schuchardt, W.A. Carvalho, E.V. Spinacé, Syn. Lett. 10 (1993) 713–718.
[2] U. Schuchardt, D. Cardoso, R. Sercheli, R. Pereira, R.S. da Cruz, M.C. Guerreiro, E.V. Spinacé, E.L. Pires, Appl. Catal. A: Gen. 211 (2001) 1–17.
[3] K.U. Ingold, Aldrichim. Acta 22 (1989) 69–73.
[4] R.A. Sheldon, J.K. Kochi, Metal-Catalyzed Oxidation of Organic Compounds, Academic Press, New York, 1981.
[5] R.P. Unnikrishan, S.D. Endalkachew, Chem. Commun. 18 (2002) 2142–2143.
[6] E.L. Pires, J.C. Magalhaes, U. Schuchardt, Appl. Catal. A: Gen. 203 (2000) 231–237.
[7] R. Zhao, D. Ji, G.A. Lv, G. Qian, L. Yan, X.L. Wang, J.S. Suo, Chem. Commun. 7 (2004) 904–905.
[8] A. Bellifa, D. Lahcene, Y.N. Tchenar, A. Choukchou-Braham, R. Bachir, S. Bedrane, C. Kappenstein, Appl. Catal. A: Gen. 305 (2006) 1–6.
[9] W.H. Yao, Y.J. Chen, L. Min, H. Fang, Z.Y. Yan, H.L. Wang, J.Q. Wang, J. Mol. Catal. A: Chem. 246 (2006) 162–166.
[10] M. Salavati-Niasari, A. Sobhani, J. Mol. Catal. A: Chem. 285 (2008) 58–67.
[11] W.A. Carvalho, P.B. Varaldo, M. Wallau, U. Schuchardt, Zeolites 18 (1997) 408–416.
[12] R.K. Rana, A.C. Pulikottil, B. Viswanathan, Stud. Surf. Sci. Catal. 113 (1998) 211–217.
[13] A. Sakthivel, P. Selvam, J. Catal. 211 (2002) 134–143.
[14] B. Retcher, J.S. Costa, J. Tang, R. Hage, P. Gamez, J. Reedijk, J. Mol. Catal. A: Chem. 286 (2008) 1–5.
[15] J. Gu, Y. Huang, S.P. Elangovan, Y. Li, W. Zhao, I. Toshino, Y. Yamazaki, J. Shi, J. Phys. Chem. C 115 (2011) 21211–21271.
[16] C. Chen, J. Xu, Q. Zhang, H. Ma, H. Miao, L. Zhou, J. Phys. Chem. C 113 (2009) 2855–2860.
[17] K. Mori, Y. Kondo, S. Morimoto, H. Yamashita, J. Phys. Chem. C 112 (2008) 397–404.
[18] Y. Du, Y. Xiong, J. Li, X. Yang, J. Mol. Catal. A: Chem. 298 (2009) 12–16.
[19] L. Satyanarayana, C.V. Gopal Reddy, S.V. Manorama, V.J. Rao, Sens. Actuators B: Chem. 46 (1998) 1–7.
[20] R.A. Canderia, M.I. Bernardi, E. Longo, I.M.G. Santosh, A.G. Souza, Mater. Lett. 58 (2004) 569–572.
[21] Y.L. Liu, Z.M. Liu, Y. Yang, H.F. Yang, G.L. Shen, R.Q. Yu, Sens. Actuators B 107 (2005) 600–604.
[22] K. Shreekumar, M. Thomas, T.M. Jyothi, M.D. Biju, S. Sugunan, B.S. Rao, Polish J. Chem. 74 (2000) 509–518.
[23] A. Walsh, Y. Yan, M.M. Al-Jassim, S.H. Wei, J. Phys. Chem. C 112 (2008) 12044–12060.
[24] G. Fierro, R. Dragone, G. Ferraris, Appl. Catal. B: Environ. 78 (2008) 183–191.
[25] G. Fierro, G. Ferraris, R. Dragone, M. Lo Jacono, M. Faticanti, Catal. Today 116 (2006) 38–49.
[26] D. Fino, N. Russo, G. Saracco, V. Spechia, J. Catal. 242 (2006) 38–49.
[27] T. Mathew, S.S. Biju, M. Devasi, M. Vijayraj Chilukuri, V.V. Satyanarayana, B.S. Rao, C.S. Gopinath, Appl. Catal. A: Gen. 273 (2004) 35–45.
[28] R. Spretz, S.G. Marchetti, M.A. Ulla, E.A. Lombordo, J. Catal. 194 (2000) 167–174.
[29] M.A. Gibson, J.W. Hightower, J. Catal. 41 (1976) 420–430.
[30] E. Manova, T. Tsoncheva, D. Paneva, I. Mitov, K. Tenchev, L. Petrov, Appl. Catal. A: Gen. 277 (2004) 119–127.
[31] L.C.A. Oliveria, J.D. Fabris, R.R.V.S. Rios, W.N. Mussel, R.M. Lago, Appl. Catal. A: Gen. 259 (2004) 253–259.
[32] S. Paldey, S. Gadevanishvii, W. Zhang, F. Rasouli, Appl. Catal. B: Environ. 56 (2005) 241–250.
[33] J.B. Silva, C.F. Diniz, R.M. Lago, N.D.S. Mohallem, J. Magn. Mater. 272–276 (2004) e1851–e1853.
[34] C.R. Xiong, Q.L. Chen, W.R. Lu, H.X. Gao, Z. Gao, Catal. Lett. 69 (2000) 231–236.
[35] F. Tihay, A.C. Roger, G. Pourroy, A. Kiennemann, Energy Fuels 16 (2002) 1271–1276.
[36] D. Guin, B. Baruwati, S.V. Manorama, J. Mol. Catal. A: Chem. 242 (2005) 26–31.
[37] N. Ma, Y. Yue, W. Hua, Z. Gao, Appl. Catal. A: Gen. 251 (2003) 39–47.
[38] W.F. Shangguan, Y. Teraoka, S. Kagawa, Appl. Catal. B: Environ. 8 (1996) 217–227.
[39] W.F. Shangguan, Y. Teraoka, S. Kagawa, Appl. Catal. B: Environ. 16 (1998) 149–154.
[40] G. Gran, Anal. Chim. Acta 14 (1956) 150–156.
[41] T. Sooknoi, J. Limtrakul, Appl. Catal. A: Gen. 233 (2002) 227–237.
[42] J. Haber, V.A. Zazhigalov, J. Stoch, L.V. Bogutskaya, I.V. Batcherikova, Catal. Today 33 (1997) 39–47.
[43] M. Abon, J.M. Herrmann, J.C. Volta, Catal. Today 71 (2001) 121–128.
[44] G.J. Hutchings, C.J. Kiely, M.T. Sananes-Schulz, A. Burrows, J.C. Volta, Catal. Today 40 (1998) 273–286.
[45] G.B. ShuÍpin, G.S. Fink, J.R.L. Smith, Tetrahedron 55 (1999) 5345–5358.
[46] A. Corma, P. Esteve, A. Martinez, J. Catal. 161 (1996) 11–19.
[47] L.X. Xu, C.H. He, M.Q. Zhu, S. Fang, Catal. Lett. 114 (2007) 202–205.
[48] M.C. Biesinger, L.W.M. Lau, A.R. Gerson, R.S.C. Smart, Appl. Surf. Sci. 257 (2010) 887–898.
[49] K.M. Parida, M. Sahoo, S. Singha, J. Mol. Catal. A: Chem. 329 (2010) 7–12.
[50] V.I. Pârvulescu, D. Dumitriu, G. Poncelet, J. Mol. Catal. A: Chem. 140 (1999) 91–105.